

Development of high- T_c SQUID microscope with flux guide*

Saburo Tanaka, Kazuka Matsuda, Osamu Yamazaki,
Miyuki Natsume, Hajime Ota and Takahiro Mizoguchi

Department of Ecological Engineering, Toyohashi University of Technology,
1-1 Hibarigaoka Tempaku-cho Toyohashi Aichi 441-8580, Japan

Received 24 July 2001, in final form 24 October 2001

Published 18 December 2001

Online at stacks.iop.org/SUST/15/146

Abstract

We have developed a new type of superconducting interference device (SQUID) microscope. A direct-coupled SQUID magnetometer with a high- μ metal needle was used and the substrate was machined to create a dimple for the needle at the centre of the pick-up loop. One end of the needle penetrated through the superconducting pick-up loop in a vacuum; the needle was fixed in the vacuum window with the other end at room temperature in the outside atmosphere. Several kinds of simulation using a Maxwell simulator were performed and the results were applied to our system. As a demonstration, a laser-printed output was scanned by the microscope. Line bars with a line width of 100 μm and a spacing between lines of 200 μm were clearly imaged.

1. Introduction

A superconducting interference device (SQUID) microscope is a powerful tool for the investigation of flux dynamics and other studies in physics [1–6]. For a low- T_c SQUID, a small transfer coil was developed and connected to the SQUID [3, 4]. However, for a high- T_c SQUID, there is no technology to transfer a small magnetic field from a small area to the SQUID. Therefore, the high- T_c SQUID must be sufficiently small and the separation of the SQUID and the sample must be as small as possible. Some groups have proposed a high- T_c SQUID microscope using a high- μ metal tip or needle to solve the above-mentioned problems [7–10]. The advantage of this system is that magnetization of the sample by the modulation coil of the SQUID can be avoided, because the coil is far enough from the sample and it is coupled not to the pick-up coil directly, but to the SQUID. Several FEED simulations have been performed. We have designed and fabricated a new type of high- T_c microscope using a fine flux guide based on the results. One end of the flux guide penetrates through the pick-up loop of the 77 K SQUID; the needle was held by the window with the other end sharpened and at room temperature. A system in which a room temperature flux guide penetrates the SQUID pick-up loop has not been reported to date. We present

a design based on a computer simulation of the magnetic field distribution and the results of the microscope.

2. Simulation

First, we investigated the feasibility of this method using computer simulations. The three-dimensional FEED electrodynamic simulation program, Maxwell (supplied by Ansoft Japan), was used. We selected a perfect conductor as the material for the pick-up loop instead of a superconductor because there was no superconducting material in the library. The permeability of the needle μ_r was selected as 60 000. The details of the simulation parameters and dimensions are shown in figure 1. One set of small-field coils with a separation of 900 μm , which generates a magnetic field of 10 mA m^{-1} , was positioned above the pick-up loop. The relative position of the set of coils and the pick-up loop was varied by steps of 150 μm in this simulation. The field calculation at the centre of the pick-up coil was performed at each position. Figure 2 shows the results of the simulation. In the case of (a) the needle penetrates through the loop. The bottom of the needle is 500 μm below the film in this case. In the case of (b) the needle is at the same level as the loop. In the case of (c) the needle is above the loop with a space of 500 μm . Two peaks, one at the position of each field coil, were observed in all the cases. However, field density in the case of (a) is the largest and one order of magnitude larger than that in the case of (c). This

* This paper was presented at the 8th International Superconductive Electronics Conference, Osaka, Japan, 19–22 June 2001.

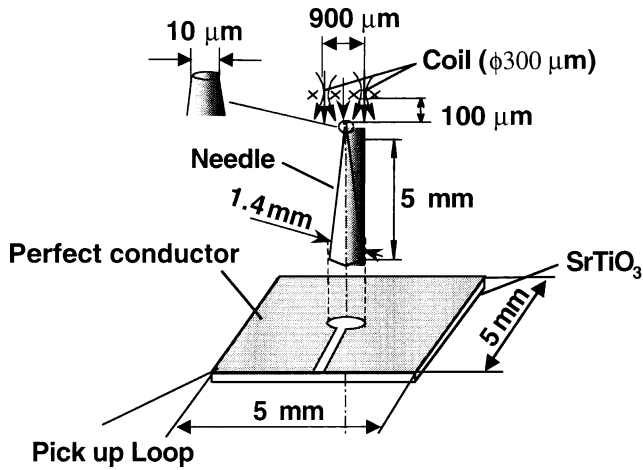


Figure 1. Model of the simulation. One set of small field coils with a separation of $900 \mu\text{m}$, which generated a magnetic field of 10 mA m^{-1} , was positioned above the pick-up loop. The relative position of the set of coils and the pick-up loop was varied by a step of $150 \mu\text{m}$ in this simulation. The separation between the top of the needle and the coil was kept constant at $100 \mu\text{m}$.

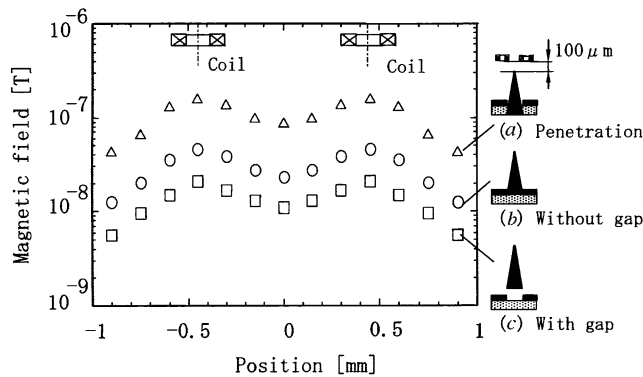


Figure 2. Effect of the position of the needle in simulation. Two peaks, one at the position of each field coil, were observed in all the cases. The field density in the case of (a) is the largest and one order of magnitude larger than that in the case of (c).

suggests that the penetration of the needle through the pick-up loop is essential to obtaining higher sensitivity.

Next we investigated the effect of the size of the top of the needle. In this simulation the space between the coil and the needle was set at $0.1 \mu\text{m}$ and the separation of the coils was $10 \mu\text{m}$ to obtain good space resolution. The results are shown in figure 3. The peaks of the field with the needle of a diameter $1 \mu\text{m}$ are sharper than those with a diameter of $10 \mu\text{m}$. This result suggests that the needle with a smaller top shows better space resolution.

3. Structure of microscope

A schematic cross-sectional view of the microscope is shown in figure 4. Most of the parts of the cryostat are made of G-10 fibreglass and Delrin [5]. The cryostat contains a liquid N_2 copper reservoir, having a volume of 0.8 litres. The inside of the cryostat can be evacuated up to the order of 10^{-3} Pa by a vacuum pump and sealed off by an o-ring valve. The SQUID chip was attached to the top of a $12 \mu\text{m}$ diameter sapphire rod with GE (General Electric Co) varnish, which was thermally

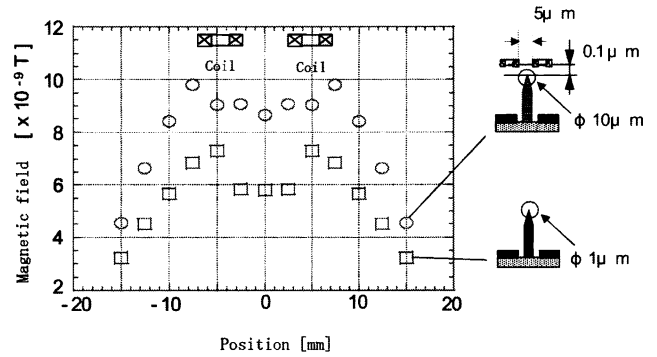


Figure 3. Effect of the size of the top of the needle in simulation. The peaks of the field with the needle of a diameter of $1 \mu\text{m}$ are sharper than those with a diameter of $10 \mu\text{m}$. This result suggests that the needle with smaller top shows a better space resolution.

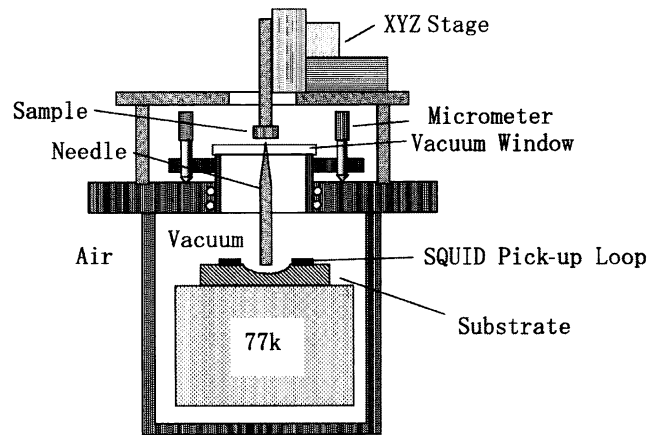


Figure 4. Schematic cross-sectional view of the SQUID microscope. The SQUID chip was on the top of a sapphire rod, which was thermally anchored with a liquid N_2 reservoir. A needle made of a high- μ metal was set at the centre of the pick-up loop. The length of the needle was 7 mm . The needle penetrated the vacuum window through a hole. Approximately $100 \mu\text{m}$ from the tip of the needle was outside of the window. The hole was sealed with silicone rubber glue after penetration.

anchored with the liquid N_2 reservoir. The SQUID was 50 mm away from the metallic reservoir. A six-turn modulation coil and a heater were installed at the upper end of the sapphire rod. A copper wire step-up transformer was glued tightly to the top of the copper reservoir. The electrical contacts to the SQUID chip were made by applying conductive silver paint to the bonding pads and the side of the SQUID chip.

A needle made of a high- μ metal (Fe-Ni base) was set at the centre of the pick-up loop. The length of the needle was 7 mm , its cross section at the bottom was a $300 \mu\text{m} \times 300 \mu\text{m}$ square shape. The top of the needle was filed so that it had a sharp edge, the shape of the top edge was not circular but oval. The size of the oval-shaped top edge was $50 \mu\text{m} \times 10 \mu\text{m}$ from microscopic observation. The needle penetrated a vacuum window through a hole and we found that about $100 \mu\text{m}$ from the top of the needle was outside the window. The hole was sealed with a silicone rubber glue after penetration. The distance between the needle and the pick-up loop was adjustable by turning $3 \mu\text{m}$.

A home-made XYZ translation stage was placed on the top plate of the cryostat. The stage was made of an

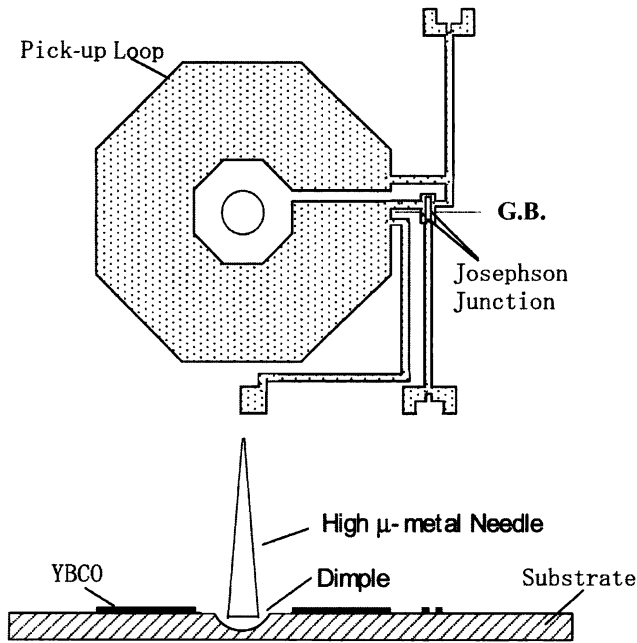


Figure 5. Schematic drawing of a directly coupled dc SQUID. The SQUID inductance was 40 pH in the calculation. The outer and inner diagonal dimensions of the pick-up loop were 6.4 mm and 2.2 mm, respectively. The substrate at the centre of the pick-up loop was machined so that a 100–200 μm deep dimple is created for the needle space.

aluminium alloy and steel and driven by an ultrasonic linear motor. The minimum step size was 0.5 μm . The translation stage was controlled by a personal computer using signals from positioning sensors. The maximum scan range was $6 \times 6 \text{ mm}^2$.

Figure 5 shows the schematic drawing of a direct-coupled dc SQUID [11]. It was made of a 200 nm thick $\text{YBa}_2\text{Cu}_3\text{O}_{7-y}$ (YBCO) thin film on a 500 μm thick SrTiO_3 substrate by sputtering. The junctions utilized in the SQUID were of 30° bi-crystal type. The inductance of the SQUID and the pick-up loop were 40 pH and 3 nH from calculations, respectively. The outer and inner diagonal dimensions of the pick-up loop were 6.4 and 2.2 mm respectively. The substrate at the centre of the pick-up loop was machined so that a 100–200 μm deep dimple was created for the needle space. It was not a through-hole but a dimple because the substrate was fragile.

4. Experimental details and discussion

The performance of the direct-coupled SQUID magnetometer was investigated. A needle was positioned at the centre of the pick-up loop. The needle was brought into contact once with the bottom of the dimple of the substrate by adjusting the micrometer and it was then lifted a little bit above the bottom for thermal isolation.

The SQUID was driven by a flux-locked loop with a flux modulation frequency of 256 kHz. The output signal from the SQUID was amplified by double transformers, one at 77 K and the other at room temperature. The R_f/M_f is $0.5 V/\phi_0$, where R_f is the feedback resistance and M_f is the mutual inductance between the SQUID magnetometer and the modulation coil. All of the measurements were performed in a magnetically shielded room, which had a shielding factor

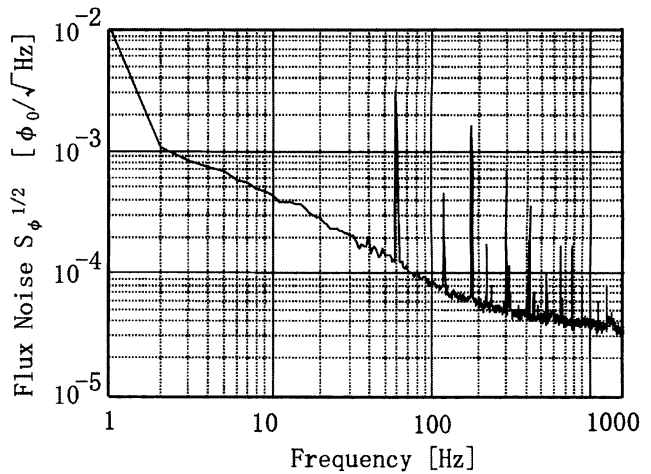


Figure 6. Flux noise of magnetometer with needle. The noise with needle was $80 \mu\phi_0/\text{Hz}^{1/2}$ at 100 Hz and $36 \mu\phi_0/\text{Hz}^{1/2}$ in the white noise region. Excess $1/f$ flux noise, which may be generated by the thermal activated hopping of vortices trapped during cooldown, was observed.

of -50 dB . A small one-turn coil with a radius of 1 mm was prepared and put on the top end of the needle to measure the local effective area at the edge of the needle. A small coil rather than a large coil was used to avoid having the field from the coil couple directly to the pick-up loop of the SQUID. A sinusoidal current of 1 $\text{mA}_{\text{p-p}}$ with a frequency of 100 Hz was used. We found that the effective area $A_{\text{eff-needle}}$ of the magnetometer was $540 \mu\text{m}^2$. This value corresponds to a small SQUID with a washer size of about $15 \mu\text{m} \times 15 \mu\text{m}$ [2]. The flux noise of the magnetometer was measured. As shown in figure 6, the noise with needle was $80 \mu\phi_0/\text{Hz}^{1/2}$ at 100 Hz and $36 \mu\phi_0/\text{Hz}^{1/2}$ in the white noise region. In contrast, the flux noise $S_\phi^{1/2}(f)$ without needle was $28 \mu\phi_0/\text{Hz}^{1/2}$ at 100 Hz. Note that the noise at around 1 Hz is not reliable because of the small number of the sampling points. Excess $1/f$ flux noise, which may be generated by the thermal-activated hopping of vortices trapped during cooldown was observed in the case with the needle. However, since the optimal bias current was not changed in the measurements with and without the needle, the trapping was not significant. A higher noise level at the white region may be due to the operation temperature of the SQUID. The temperature at the top of the sapphire rod is about 2–3 K higher than the liquid nitrogen boiling point.

Laser-printed outputs were used as a sample to test the microscope. Laser printer ink contains ferromagnetic particles and therefore it is easy to generate a bar line. The finest pattern we prepared was a line width of 100 μm and a spacing of 200 μm between lines. This pattern was restricted by the resolution of the laser printer. The samples were moved in the direction in which the needle crosses the bar lines. The XY translation stage was not used in this experiment; however, a pattern was made from a thin string drawn by a miniature induction motor installed outside of the magnetically shielded room. The schematic drawing of this scanning is shown in figure 7(a). The upper figure shows the top view and the lower shows the side view. The figure in the middle depicts the shape of the top edge of the needle. The scanning direction was along the longer axis of the oval top edge. The velocity

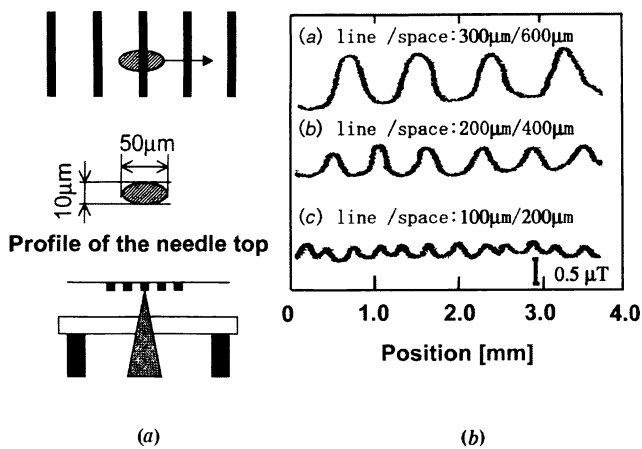


Figure 7. Results of the scanning. (a) Schematic drawing of the scanning configuration and (b) the output signal of the SQUID when laser-printed bar patterns were scanned. The finest pattern we prepared was a line width of $100 \mu\text{m}$ and a spacing of $200 \mu\text{m}$ between lines.

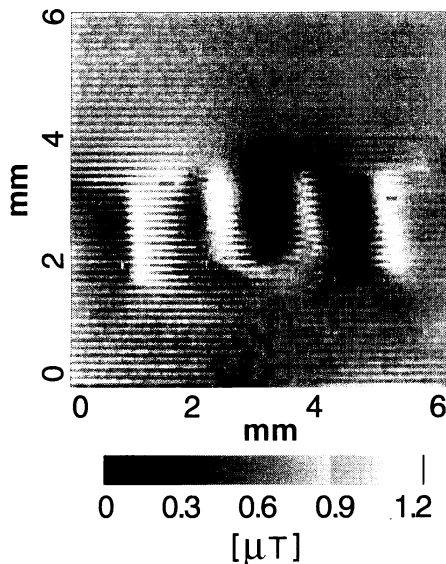


Figure 8. Two-dimensional magnetic field image of the printed pattern of the characters TUT.

of the scanning was $620 \mu\text{m s}^{-1}$. The surface of the sample was brought into contact with the end of the needle during the scan. Figure 7(b) shows the output signal of the SQUID. The signal was measured through a low pass filter of 5 kHz. All the patterns were clearly observed. The peak-peak value of the signal that corresponds to the line was about $0.15 \mu\text{T}$. Therefore this system has at least a resolution of line/space = $100 \mu\text{m}/200 \mu\text{m}$.

Next we raster-scanned the printed output pattern of the characters 'TUT' using the XYZ translation stage. It took 150 s to scan the $6 \text{ mm} \times 6 \text{ mm}$ area. The signals in the bandwidth range of 0.8 Hz to 5 kHz were measured to eliminate the background field. The step sizes were $2 \mu\text{m}$ in the x direction and $20 \mu\text{m}$ in the y direction. The separation between the sample and the end of the needle was adjusted to be about $100 \mu\text{m}$ to avoid friction between the sample and the needle edge. Figure 8 shows the obtained image. Inhomogeneity of the line-to-space ratio is due to the quality of the laser-printed patterns. The image was in good agreement with the sample.

5. Conclusion

In conclusion, we have designed and constructed a new type of magnetic microscope using a high- T_c SQUID with a room temperature, high- μ metal needle. One end of the needle penetrated a superconducting pick-up loop in a vacuum; the needle was fixed in the vacuum window with the other end at room temperature in the outside atmosphere. Using a FEED electrodynamic simulation, it was found that when the needle penetrated the superconducting loop, the magnetic field density at the loop was one order of magnitude larger than that in the case of no penetration. Therefore, the substrate of a direct-coupled SQUID magnetometer was machined to create a dimple at the centre of the pick-up loop to provide room for the needle. Laser-printed output was scanned by the microscope. Line bars with a line width of $100 \mu\text{m}$ and a spacing between lines of $200 \mu\text{m}$ were clearly imaged. Since the top edge of the smaller needle showed better spatial resolution in our simulations, the space resolution can be improved by using a sharper needle edge.

Acknowledgment

This work was partially supported by a grant-in-aid for Scientific Research in Priority Area (A) from the Ministry of Education, Culture, Sports, Science and Technology.

References

- [1] Black R C, Mathai A, Wellstood F C, Dantsker E, Miklich A H, Nemeth D T, Kingston J J and Clarke J 1993 Magnetic microscopy using a liquid nitrogen cooled $\text{YBa}_2\text{Cu}_3\text{O}_7$ superconducting quantum interference device *Appl. Phys. Lett.* **62** 2128
- [2] Lee T S, Dantsker E and Clarke J 1996 High-transition temperature superconducting quantum interference device microscope *Rev. Sci. Instrum.* **67** 4208
- [3] Kirtley J R, Ketchen M B, Stawiasz K G, Sun J Z, Gallagher W J, Blanton S H and Wind S J 1995 High-resolution scanning SQUID microscope *Appl. Phys. Lett.* **66** 1138
- [4] Morooka T, Nakayama S, Odawara A, Ikeda M, Tanaka S and Chinone K 1999 Micro-imaging system using scanning DC-SQUID microscope *IEEE Trans. Appl. Supercond.* **9** 3491
- [5] Tanaka S, Yamazaki O, Shimizu R and Saito Y 1999 High- T_c SQUID microscope with sample chamber *Supercond. Sci. Technol.* **12** 809
- [6] Fleet E F, Chatrathorn S, Wellstood F C and Knauss L A 1999 HTS scanning SQUID microscopy of active circuits *IEEE Trans. Appl. Supercond.* **9** 4103
- [7] Pitzius P, Dworak V and Hartmann U 1997 Ultrahigh-resolution scanning SQUID microscopy *6th Int. Supercond. Electronics Conf. (ISEC'97) Extended Abstracts* **3** 395
- [8] Tavrin Y and Seigel M 1998 New type of HTS-SQUID microscope without shielding *Appl. Supercond.* **1** 719
- [9] Nagaishi T, Minamimura K and Itozaki H 2001 HTS SQUID microscope head with sharp permalloy rod for high spatial resolution *IEEE Trans. Appl. Supercond.* **11** 226
- [10] Gudoshnikov S A, Deryuzhkina Y V, Rudenchik P E, Sintnov Y S, Bondarenko S I, Shablo A A, Pavlov P P, Kalabukhova A S, Snigirev O V and Seidel P 2001 Magnetic flux guide for high-resolution SQUID microscope *IEEE Trans. Appl. Supercond.* **11** 219
- [11] Tanaka S, Matsuda K, Yamazaki O, Natsume M, Ota H and Mizoguchi T 2001 Properties of high T_c superconducting quantum interference device microscope with high- μ metal needle *Japan J. Appl. Phys.* **40** L431